Hindawi Publishing Corporation
International Journal of Antennas and Propagation
Volume 2015, Article ID 539843, 7 pages
http://dx.doi.org/10.1155/2015/539843

Research Article

Wearable Fabric Reconfigurable Beam-Steering Antenna for On/Off-Body Communication System

Seonghun Kang and Chang Won Jung

Graduate School of NID Fusion Technology, Seoul National University of Technology, 172 Gongneung 2-dong, Nowon-gu, Seoul 139-743, Republic of Korea

Correspondence should be addressed to Chang Won Jung; changwoj@snut.ac.kr

Received 20 October 2014; Revised 12 December 2014; Accepted 29 December 2014

Academic Editor: N. Nasimuddin

This paper presents a comparison of on-body performances between omnidirectional (loop antenna) and reconfigurable beam-steering antennas. Both omnidirectional and reconfigurable antennas were manufactured on the same fabric substrate and operated at the frequency band of the WLAN 802.11a (5.725–5.85 GHz). The reconfigurable antenna was designed to steer the beam directions. In order to implement the beam-steering capability, the antenna used two PIN diodes. The maximum beam directions of three states (states 0, 1, and 2) were steerable in the YZ-plane (h = 2°, 28°, and 326°, resp.). The measured peak gains were 5.9–6.6 dBi and the overall half power beam width (HPBW) was 102°. The measured results of total radiated power (TRP) and total isotropic sensitivity (TIS) indicated that the communication efficiency of the reconfigurable beam steering antenna was better than that of the loop antenna. When the input power was 0.04 W (16 dBm), the simulated specific absorption rate (SAR) values of the reconfigurable beam steering antenna on the body were less than 0.979 W/kg (1 g tissue) in all states, satisfying the SAR criteria of the US.

1. Introduction

In recent years, the growing interest in antennas with wearable applications in clothing has led to a wide range of wireless body-centric system applications [1]. One of the dominant research topics in antennas for body-centric communications is wearable, fabric-based antennas [2]. Wearable antennas need to have the characteristics of small size, low profile, and low mutual influence between antennas and the human body for high antenna efficiency and a low specific absorption rate (SAR) [3, 4]. Since wearable antenna in presence of the body has flexibility due to the motion of the human, beam-steering capability is required to change the radiation pattern and enhance the directivity in the desired directions [5]. Beam-steering antennas are mostly classified as either adaptive array antennas (AAAs) or single reconfigurable antennas (SRAs). SRAs provide several advantages, such as simple design, small size, and easy radiation handling as compared to AAAs. Since AAAs are larger and more complex because of the use of several antenna elements and phase shifters, it is preferable to use SRAs for integration into clothing [5–7]. In a previous work, we proposed reconfigurable beam-steering by means of a microstrip patch antenna with a U-slot for wearable fabric applications [5]. This antenna employed two PIN diodes to obtain beam-steering capability.

In this paper, a reconfigurable beam-steering antenna with WLAN 802.11a (5.725–5.85 GHz) was designed and fabricated. The antenna is able to steer the maximum beam direction in the YZ-plane. The simulated and measured results of radiation patterns confirmed that steering characteristics can be realized using two PIN diodes. This antenna was compared in terms of on-body performance with a loop antenna as an omnidirectional antenna. In other words, to compare the communication efficiency of the two antennas, we measured total radiated power (TRP) and total isotropic sensitivity (TIS). In addition, we performed simulations in terms of the SAR in order to compare the antenna's influences in the vicinity of the human body and to analyze the SAR values between the two antennas.

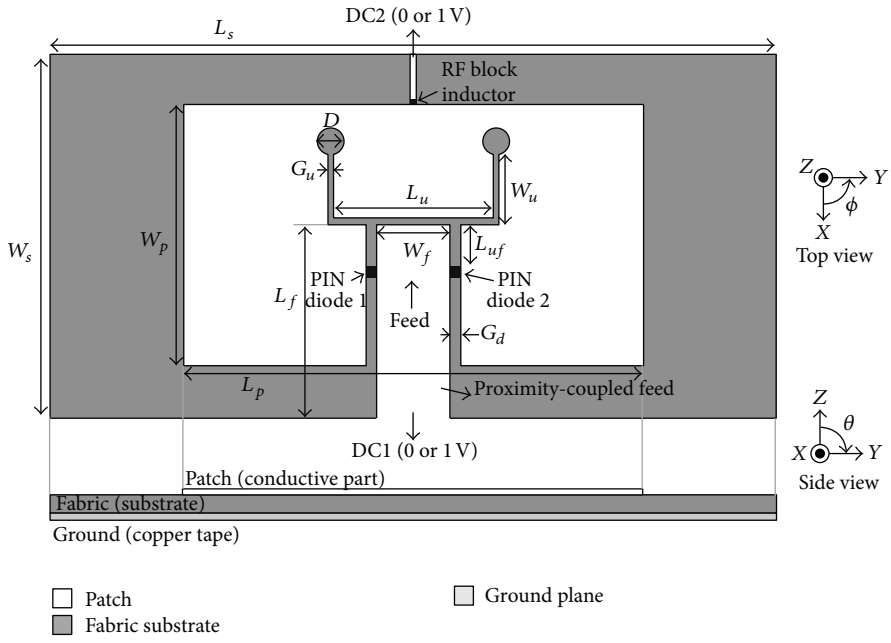

Figure 1: Configuration of the reconfigurable beam-steering antenna.

2. Design and Configuration of the Omni and Beam-Steering Antennas on a Fabric Substrate

The geometry of the proposed configuration of the reconfigurable beam-steering antenna is shown in Figure 1. This antenna was fabricated on a fabric substrate which is consisted of polyester 66.2% and cotton 33.8% with a thickness of 1.5 mm, relative permittivity of 1.35, and loss tangent of 0.02. The loss tangent is typically applied when discussing dielectric materials, for which a small value is desirable [8]. Because loss tangent of the fabric material is low, the substrate has minimal losses. A patch and a ground were positioned on the front and back of the substrate. The antenna patch which is polyester (PES) #3 (ε_r = 4.0 and $\tan\delta$ = 0.02, thickness = 0.14 mm) was manufactured with silver paste to maintain its flexibility. The silver paste was a mixture of silver powder and acrylic resin. The detailed fabrication process of the proposed antenna is as follows. The conductive ink as silver paste is used in screen-printing due to its high conductivity and adhesivity to the fabrics. The standard screen printing process is comprised of printing, drying, and firing. The conductive ink is painted through the open areas of a mesh-reinforced stencil onto the fabric substrate as in the common silk screening process, and alignment for geometric accuracy can be achieved with common screen printing equipment. The firing process is performed below 150°C for 20–30 min to avoid the deformation of the fabric substrate. Next, the patch as CP (conductive part) is cut according to the dimension of the patch antenna and attached with substrate as FP (fabric part) using an adhesive [9]. The ground was manufactured with copper and consisted of the bottom plane to avoid affecting electromagnetic waves in the human body.

The overall dimensions of the proposed antenna are given in Table 1. The configuration of the proposed the loop antenna, which was fabricated on the same fabric substrate, is shown in Figure 2. The antenna loop was also manufactured with silver paste. The overall dimensions of the loop antenna are given in Table 2. In order to realize beam-steering in the proposed antenna, two PIN diodes (Microsemi's MPP4203) were used. The RF equivalent circuit of the PIN diode is shown in Figure 3. In the On-state (forward bias), the PIN diode mainly behaves as a current-controlled resistor, which is expressed by a series resistor (R_S) connected in series with a fixed inductor (L). Also, in the Off-state (reverse bias), the equivalent circuit consists of the shunt combination of the intrinsic-layer capacitance (C_R) and the parallel resistance (R_S) in series with the fixed inductance (L). We used the PIN diodes to check the performance. The value of C_R (0.1 pF) was presented in the Off-state. The value of L (0.2 nH) in both states was the same. But, the value of R_S (3 Ω) in the On-state was much lower than that of R_S (100 kΩ) in the Off-state [10]. The antenna patch and the proximity-coupled feed were designed to be connected using the two PIN diodes. The two PIN diodes, which were configured with just a line connection, were located between the feeding line and the antenna patch to control the current distributions and could be controlled by two DC bias inputs (DC1 and DC2). In order to miniaturize the system and obtain a wide-band frequency range, a U-slot structure was used. There were three states (states 0, 1, and 2) created by using two PIN diodes, as shown in Table 3. The DC1 input was biased through antenna feed. The DC2 input was connected with the antenna patch through an RF block inductor (Samsung's 0603) at the top of antenna and could supply 0 or 1 (V).

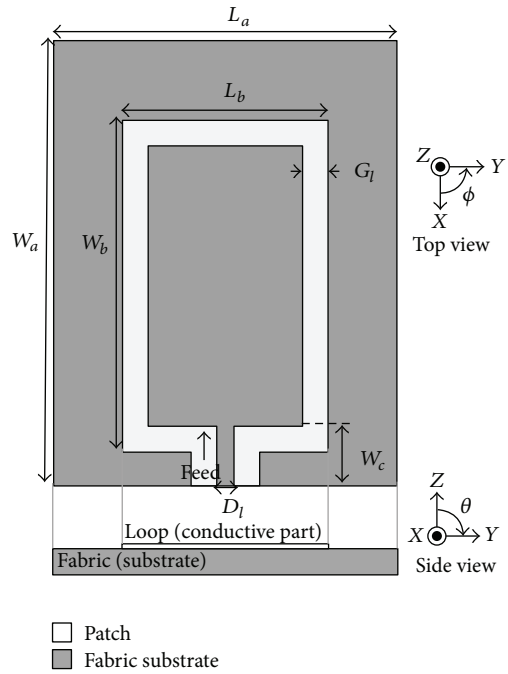

Figure 2: Configuration of the loop antenna.

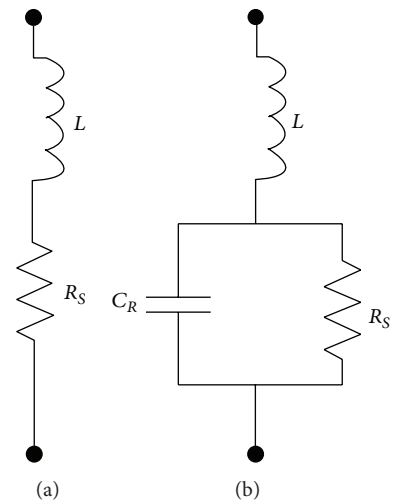

Figure 3: Equivalent circuit of a packaged PIN diode in its two-bias conditions: (a) *On-state* (forward bias) and (b) *Off-state* (reverse bias).

Table 1: Dimensions of the reconfigurable beam-steering antenna.

Parameter	L_s	W_s	L_p	W_p	L_f	W_f
Unit (mm)	60	30	38	21.3	16	6.04
Parameter	L_u	W_u	L_{uf}	G_u	G_d	D
Unit (mm)	13.1	6.0	3.5	0.5	0.9	2.2

Table 2: Dimensions of the loop antenna.

Parameter	L_a	W_a	L_b	W_b	W_c	D_l	G_l
Unit (mm)	20	26	12	19.4	3.5	1	1.5

Table 3: State configurations by PIN diodes and DC biasing.

State	PIN diode 1	PIN diode 2	DC 1 (V)	DC 2 (V)
State 0	On	Off	0	0
State 1	On	On	1	0
State 2	Off	On	0	1

3. Simulation and Measurement Result of the Omni and Beam-Steering Antennas on a Fabric Substrate

The measured reflection coefficients of the proposed antenna on the human body phantom by the three states (states 0, 1,

Table 4: Summary of the measured antenna performances.

State	Bandwidth (GHz)	Maximum beam direction (°)		HPBW (°)	Peak gain (dBi)
		ϕ	θ		
State 0	5.69–5.96	0	2	60	5.9
State 1	5.51–6.05	90	28	63	6.59
State 2	5.43–6.03	270	326	64	6.64
Loop	5.27–6.22	0	0	42	4.46

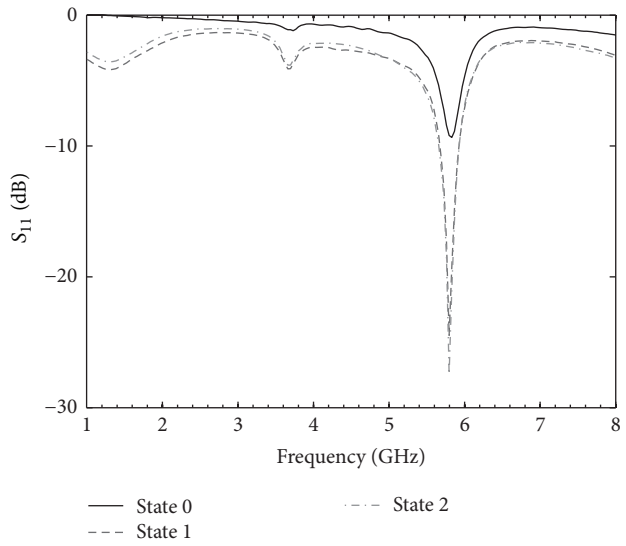

Figure 4: Measured S_{11} of the reconfigurable beam-steering antenna.

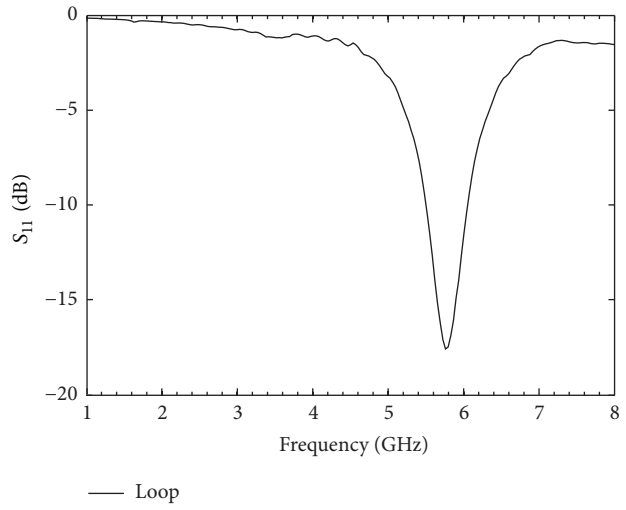

Figure 5: Measured S_{11} of the loop antenna.

and 2) are shown in Figure 4. All the reflection coefficients were under −6 dB (VSWR < 3) at an operation frequency band. The operation bandwidth of state 0 is 5.69–5.96 GHz, state 1 is 5.51–6.05 GHz, and state 2 is 5.43–6.03 GHz. The measured reflection coefficients of the loop antenna on the human body phantom are shown in Figure 5. The reflection coefficients of the antenna was under −6 dB at the operation frequency band of 5.27–6.22 GHz. Figures 6 and 7 show the simulated three-dimensional radiation patterns (YZ-plane) of the proposed antenna and the loop antenna at 5.8 GHz using an HFSS software. The maximum beam directions of the radiation patterns were clearly changed by the states (states 0, 1, and 2). Figure 8 shows the measured two-dimensional radiation patterns on the human body phantom in the YZ-plane (θ) at 5.8 GHz. The measured maximum beam direction, peak gain, and half power beam width (HPBW) of the proposed antenna's three states and the loop antenna are summarized in Table 4. These results indicate that the reconfigurable beam-steering antenna is able to steer beam direction and has high gain in comparison with the loop antenna. Figure 9 shows photographs of two fabricated antennas with the WLAN module on the human body phantom (SPEAG's TORSO-OTA-V5.1).

4. Performance Comparison of the TRP/TIS/SAR of the Omni/Beam-Steering Antennas

A system diagram of measuring TRP/TIS in the chamber is shown in Figure 10. To measure TRP/TIS, the proposed antenna had been linked to a WLAN 802.11a modem. The modem had been connected to a laptop computer. The laptop computer controlled the status of the modem. The modem was access point (AP) state and channel 153 (center freq. = 5.785 GHz). A communication tester (R&S CMW270) for WiBro/WiMAX set up same channel with the modem. A horn antenna was linked to a vector signal generator (Agilent E4438C) and a communication tester. The proposed antenna, the modem, and the laptop computer are situated on the test position using a Zig. When the measurements were running, the values of TRP/TIS are measured through transmitting and receiving signals between the proposed antenna and a horn antenna in the chamber. Figures 11 and 12 present the TRP and TIS. The figures show TRP/TIS according to the YZ-plane (θ). In state 0, the maximum TRP/TIS direction was $\theta = 0^\circ$ and the values were 24 dBm and −79 dBm, respectively. In state 1, the maximum TRP/TIS direction was $\theta = 30^\circ$ and the values were 25 dBm and −79 dBm, respectively. In state 2, the maximum TRP/TIS direction was $\theta = 330^\circ$ and the values were 23 dBm and −78 dBm, respectively. In the loop antenna, the maximum TRP/TIS direction was $\theta = 0^\circ$ and the values were 22 dBm and −77 dBm, respectively. Comparing Figure 8 with Figures 11 and 12, maximum beam direction in Figure 8 and maximum TRP/TIS direction in Figures 11 and 12 were

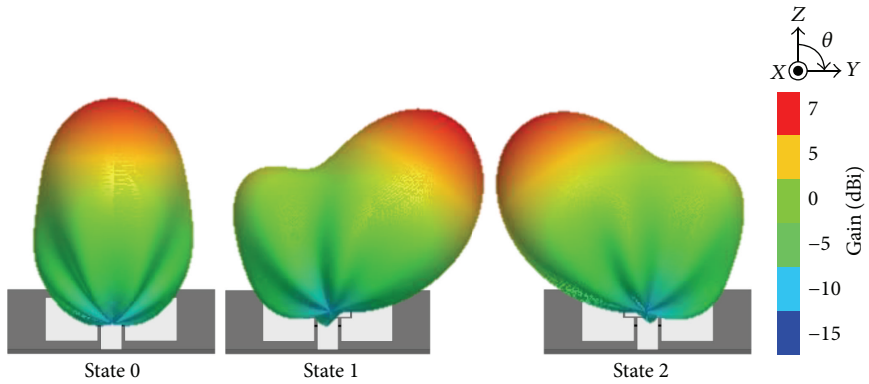

Figure 6: Simulated three-dimensional radiation patterns of the reconfigurable beam-steering antenna.

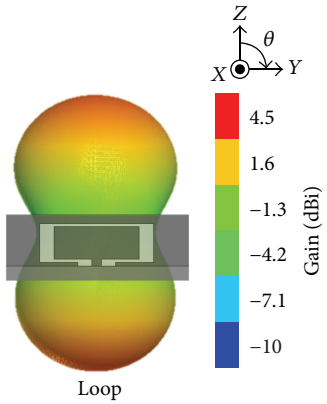

Figure 7: Simulated three-dimensional radiation patterns of the loop antenna.

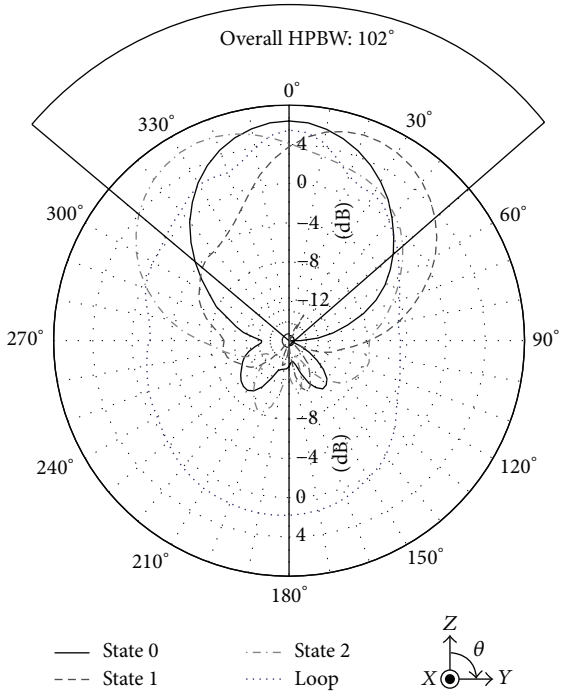

Figure 8: Measured radiation patterns of the proposed antenna's three states (states 0, 1, and 2) and the loop antenna at 5.8 GHz.

Table 5: Summary of the simulated peak SAR values.

State	Peak SAR values (W/kg)	
	1 g tissue (US standard)	10 g tissue (EU standard)
State 0	0.681	0.093
State 1	0.979	0.161
State 2	0.924	0.158
Loop	4.216	0.743

the same. The mean of the beam tilt angles was also the same. The measured TRP/TIS values of the proposed antenna (state 0, 1, and 2) were higher than loop antenna. The value of the SAR is an essential factor in evaluating the antenna's effect in the vicinity of the human body for on-body applications. The simulation was therefore carried out in the condition of the antenna contacting a human chest at 5.8 GHz, as shown in Figure 13. The simulation tools comprised of SEMCAD X and the human model software of the Information Technologies in Society (IT'IS) Foundation. The information of this human model is as follows: relative permittivity (ε_r) is 35.36 and loss tangent ($\tan\delta$) is 0.32. The level of input power was 0.04 W (16 dBm). The IEEE standard requires a level below 1.6 W/kg over a volume of 1 g of tissue, while the International Commission on NonIonizing Radiation Protection standard requires 2 W/kg over a volume of 10 g of tissue. The peak SAR values of the proposed antenna were 0.68–0.98 W/kg (1 g tissue) and 0.09–0.16 W/kg (10 g tissue). The peak SAR values of the loop antenna were 4.22 W/kg (1 g tissue) and 0.74 W/kg (10 g tissue). The simulated peak SAR values are summarized in Table 5. We confirmed that the reconfigurable beam-steering antenna satisfies the IEEE standard SAR values, but the loop antenna does not.

5. Conclusions

In this paper, the performances of a reconfigurable beam-steering antenna on a wearable fabric substrate were simulated, measured, and compared with a loop antenna as an omnidirectional antenna. The operation frequency band

(a) (b)

Figure 9: Photographs of two fabricated antennas with the WLAN module on the human body phantom: (a) reconfigurable beam-steering antenna, (b) loop antenna.

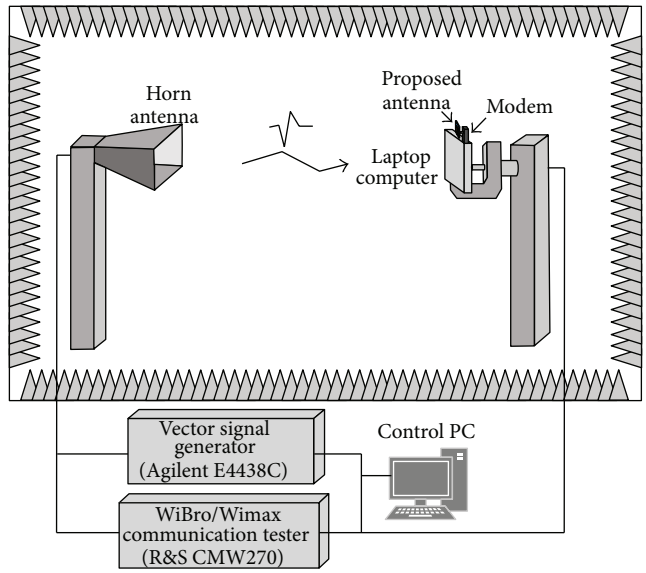

Figure 10: System diagram of measuring TRP/TIS in the chamber.

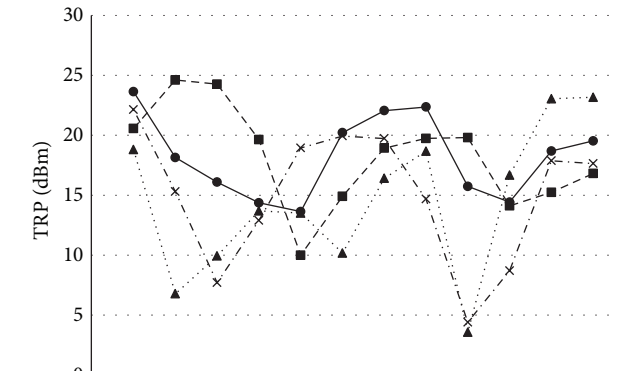

θ	0°	30°	60°	90°	120°	150°	180°	210°	240°	270°	300°	330°
State 0	24	18	16	14	14	20	22	22	16	14	19	20
State 1	21	25	24	20	10	15	19	20	20	14	15	17
State 2	19	7	10	14	14	10	16	19	4	17	23	23
Loop	22	15	8	13	19	20	20	15	4	9	18	18

Figure 11: Measured total radiated power (TRP) of the antenna.

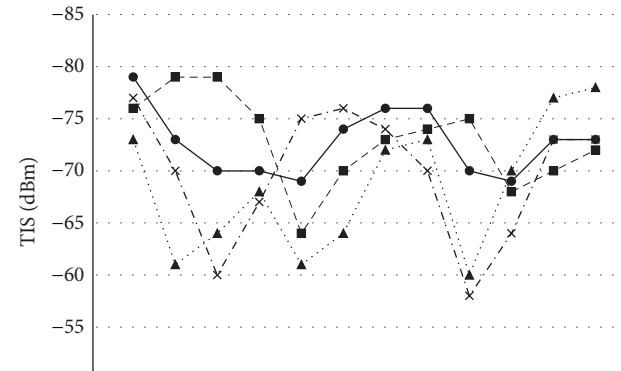

θ	0°	30°	60°	90°	120°	150°	180°	210°	240°	270°	300°	330°
State 0	−79	−73	−70	−70	−69	−74	−76	−76	−70	−69	−73	−73
State 1	−76	−79	−79	−75	−64	−70	−73	−74	−75	−68	−70	−72
State 2	−73	−61	−64	−68	−61	−64	−72	−73	−60	−70	−77	−78
Loop	−77	−70	−60	−67	−75	−76	−74	−70	−58	−64	−73	−73

Figure 12: Measured total isotropic sensitivity (TIS) of the antenna.

Figure 13: Simulated SAR values of two antennas on the body at 5.8 GHz: (a) reconfigurable beam-steering antenna, (b) loop antenna.

of the two antennas was the WLAN 802.11a band (5.725–5.85 GHz). The measured results demonstrated that the proposed antenna had high gain and a low SAR in comparison with the loop antenna. In addition, measurements of the TRP/TIS showed that the communication efficiency of the proposed antenna was better than that of the loop antenna. Therefore, the reconfigurable beam-steering antenna with a single antenna has a variety of advantages in on/off-body communication systems.

Conflict of Interests

The authors certify that there is no conflict of interests with any financial organization regarding the material discussed in the paper.

Acknowledgments

This work was supported in part by the IT R&D Program of MKE/KEIT (10041145, Self-Organized Software-platform (SOS) for welfare devices) and in part by the BK 21 Plus project by NRF Korea.

References

[1] P. Salonen and Y. Rahmat-Samii, "Wearable antennas: advances in the design, characterization and application," in *Antennas and Propagation for Body-Centric Wireless Communications*, P. Hall and Y. Hao, Eds., pp. 151–188, Artech House, Norwood, Mass, USA, 2006.

[2] N. H. M. Rais, P. J. Soh, F. Malek, S. Ahmad, N. B. M. Hashim, and P. S. Hall, "A review of wearable antenna," in *Proceedings of the IEEE Antennas & Propagation Conference*, pp. 225–228, Loughborough, UK, November 2009.

[3] N. Haga, K. Saito, M. Takahashi, and K. Ito, "Characteristics of cavity slot antenna for body-area networks," *IEEE Transactions on Antennas and Propagation*, vol. 57, no. 4, pp. 837–843, 2009.

[4] S. Kim, K. Kwon, and J. Choi, "Design of a miniaturized high-isolation diversity antenna for wearable WBAN applications," *Journal of Electromagnetic Engineering and Science*, vol. 13, no. 1, pp. 28–33, 2013.

[5] S.-J. Ha and C. W. Jung, "Reconfigurable beam steering using a microstrip patch antenna with a U-slot for wearable fabric applications," *IEEE Antennas and Wireless Propagation Letters*, vol. 10, pp. 1228–1231, 2011.

[6] H. A. Majid, M. K. A. Rahim, M. R. Hamid, and M. F. Ismail, "Frequency and pattern reconfigurable YAGI antenna," *Journal of Electromagnetic Waves and Applications*, vol. 26, no. 2-3, pp. 379–389, 2012.

[7] M. F. Jamlos, O. A. Aziz, T. A. Rahman et al., "A beam steering radial line slot array (RLSA) antenna with reconfigurable operating frequency," *Journal of Electromagnetic Waves and Applications*, vol. 24, no. 8-9, pp. 1079–1088, 2010.

[8] S. M. Wentworth, *Fundamentals of Electromagnetics with Engineering Applications*, John Wiley & Sons, 2005.

[9] S.-J. Ha, Y.-B. Jung, D. H. Kim, and C. W. Jung, "Textile patch antennas using double layer fabrics for wrist-wearable applications," *Microwave and Optical Technology Letters*, vol. 54, no. 12, pp. 2697–2702, 2012.

[10] I. Yeom, J. Choi, S.-S. Kwoun, B. Lee, and C. Jung, "Analysis of RF front-end performance of reconfigurable antennas with RF switches in the far field," *International Journal of Antennas and Propagation*, vol. 2014, Article ID 385730, 14 pages, 2014.